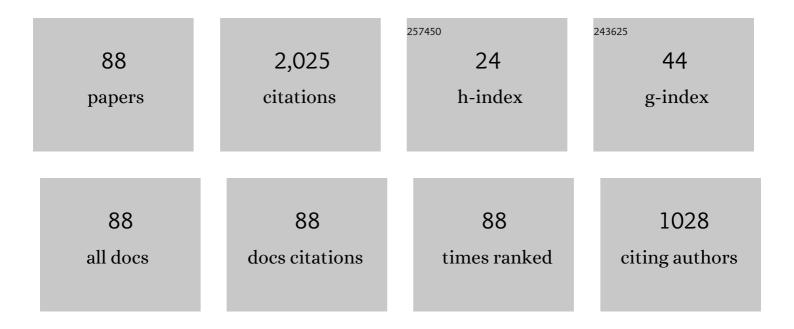
Biao Zhang

List of Publications by Year in descending order

Source: https://exaly.com/author-pdf/750759/publications.pdf Version: 2024-02-01



<u>Βιλο Ζηλης</u>

#	Article	IF	CITATIONS
1	Cross-Polarized Synthetic Aperture Radar: A New Potential Measurement Technique for Hurricanes. Bulletin of the American Meteorological Society, 2012, 93, 531-541.	3.3	189
2	Mapping sea surface oil slicks using RADARSAT-2 quad-polarization SAR image. Geophysical Research Letters, 2011, 38, n/a-n/a.	4.0	148
3	Wind speed retrieval from RADARSAT-2 quad-polarization images using a new polarization ratio model. Journal of Geophysical Research, 2011, 116, .	3.3	118
4	Combined Co- and Cross-Polarized SAR Measurements Under Extreme Wind Conditions. IEEE Transactions on Geoscience and Remote Sensing, 2017, 55, 6746-6755.	6.3	116
5	Ocean Vector Winds Retrieval From C-Band Fully Polarimetric SAR Measurements. IEEE Transactions on Geoscience and Remote Sensing, 2012, 50, 4252-4261.	6.3	113
6	A Hurricane Wind Speed Retrieval Model for C-Band RADARSAT-2 Cross-Polarization ScanSAR Images. IEEE Transactions on Geoscience and Remote Sensing, 2017, 55, 4766-4774.	6.3	87
7	High-Resolution Hurricane Vector Winds from C-Band Dual-Polarization SAR Observations. Journal of Atmospheric and Oceanic Technology, 2014, 31, 272-286.	1.3	86
8	Comparison of composite Bragg theory and quadâ€polarization radar backscatter from RADARSATâ€2: With applications to wave breaking and high wind retrieval. Journal of Geophysical Research, 2010, 115,	3.3	83
9	Crossâ€polarization geophysical model function for Câ€band radar backscattering from the ocean surface and wind speed retrieval. Journal of Geophysical Research: Oceans, 2015, 120, 893-909.	2.6	79
10	Copolarized and Crossâ€Polarized SAR Measurements for Highâ€Resolution Description of Major Hurricane Wind Structures: Application to Irma CategoryÂ5 Hurricane. Journal of Geophysical Research: Oceans, 2019, 124, 3905-3922.	2.6	68
11	Depolarized radar return for breaking wave measurement and hurricane wind retrieval. Geophysical Research Letters, 2010, 37, .	4.0	60
12	Oceanic Eddy Characteristics and Generation Mechanisms in the Kuroshio Extension Region. Journal of Geophysical Research: Oceans, 2018, 123, 8548-8567.	2.6	56
13	A C-Band Geophysical Model Function for Determining Coastal Wind Speed Using Synthetic Aperture Radar. IEEE Journal of Selected Topics in Applied Earth Observations and Remote Sensing, 2018, 11, 2417-2428.	4.9	55
14	Upper Ocean Response to Typhoon Kalmaegi and Sarika in the South China Sea from Multiple-Satellite Observations and Numerical Simulations. Remote Sensing, 2018, 10, 348.	4.0	47
15	Rain effects on the hurricane observations over the ocean by Câ€band Synthetic Aperture Radar. Journal of Geophysical Research: Oceans, 2016, 121, 14-26.	2.6	43
16	Ship Detection Using a Fully Convolutional Network with Compact Polarimetric SAR Images. Remote Sensing, 2019, 11, 2171.	4.0	42
17	Bridging the gap between cyclone wind and wave by <scp>C</scp> â€band <scp>SAR</scp> measurements. Journal of Geophysical Research: Oceans, 2017, 122, 6714-6724.	2.6	41
18	A New Algorithm to Retrieve Wave Parameters From Marine X-Band Radar Image Sequences. IEEE Transactions on Geoscience and Remote Sensing, 2014, 52, 4083-4091.	6.3	36

#	Article	IF	CITATIONS
19	On Quad-Polarized SAR Measurements of the Ocean Surface. IEEE Transactions on Geoscience and Remote Sensing, 2019, 57, 8362-8370.	6.3	34
20	A Geophysical Model Function for Wind Speed Retrieval From C-Band HH-Polarized Synthetic Aperture Radar. IEEE Geoscience and Remote Sensing Letters, 2019, 16, 1521-1525.	3.1	31
21	Compact Polarimetric Synthetic Aperture Radar for Marine Oil Platform and Slick Detection. IEEE Transactions on Geoscience and Remote Sensing, 2017, 55, 1407-1423.	6.3	30
22	A novel deep learning method for marine oil spill detection from satellite synthetic aperture radar imagery. Marine Pollution Bulletin, 2022, 179, 113666.	5.0	30
23	Synergistic measurements of ocean winds and waves from SAR. Journal of Geophysical Research: Oceans, 2015, 120, 6164-6184.	2.6	29
24	A Method to Correct the Influence of Rain on X-Band Marine Radar Image. IEEE Access, 2017, 5, 25576-25583.	4.2	26
25	Validation of RADARSATâ€2 fully polarimetric SAR measurements of ocean surface waves. Journal of Geophysical Research, 2010, 115, .	3.3	24
26	Recent progress on high wind-speed retrieval from multi-polarization SAR imagery: a review. International Journal of Remote Sensing, 2014, 35, 4031-4045.	2.9	24
27	Inconsistencies in scatterometer wind products based on ASCAT and OSCAT-2 collocations. Remote Sensing of Environment, 2019, 225, 207-216.	11.0	23
28	A Hurricane Tangential Wind Profile Estimation Method for C-Band Cross-Polarization SAR. IEEE Transactions on Geoscience and Remote Sensing, 2014, 52, 7186-7194.	6.3	22
29	An Automatic Algorithm to Retrieve Wave Height From X-Band Marine Radar Image Sequence. IEEE Transactions on Geoscience and Remote Sensing, 2017, 55, 5084-5092.	6.3	22
30	Estimation of Wind Direction in Tropical Cyclones Using C-Band Dual-Polarization Synthetic Aperture Radar. IEEE Transactions on Geoscience and Remote Sensing, 2020, 58, 1450-1462.	6.3	22
31	Application of AMSR-E and AMSR2 Low-Frequency Channel Brightness Temperature Data for Hurricane Wind Retrievals. IEEE Transactions on Geoscience and Remote Sensing, 2016, 54, 4501-4512.	6.3	17
32	Examination of Surface Wind Asymmetry in Tropical Cyclones over the Northwest Pacific Ocean Using SMAP Observations. Remote Sensing, 2019, 11, 2604.	4.0	16
33	Retrieving Hurricane Wind Speed From Dominant Wave Parameters. IEEE Journal of Selected Topics in Applied Earth Observations and Remote Sensing, 2017, 10, 2589-2598.	4.9	15
34	Remote sensing of ocean waves by alongâ€ŧrack interferometric synthetic aperture radar. Journal of Geophysical Research, 2009, 114, .	3.3	12
35	Estimating Tropical Cyclone Wind Structure and Intensity From Spaceborne Radiometer and Synthetic Aperture Radar. IEEE Journal of Selected Topics in Applied Earth Observations and Remote Sensing, 2021, 14, 4043-4050.	4.9	12
36	Ku-Band Sea Surface Radar Backscatter at Low Incidence Angles under Extreme Wind Conditions. Remote Sensing, 2017, 9, 474.	4.0	11

#	Article	IF	CITATIONS
37	Retrievals of sea surface temperature fronts from SAR imagery. Geophysical Research Letters, 2012, 39,	4.0	10
38	Investigation of sea level variability in the Baltic Sea from tide gauge, satellite altimeter data, and model reanalysis. International Journal of Remote Sensing, 2015, 36, 2548-2568.	2.9	10
39	A new modulation transfer function for ocean wave spectra retrieval from X-band marine radar imagery. Chinese Journal of Oceanology and Limnology, 2015, 33, 1132-1141.	0.7	10
40	An oceanic eddy statistical comparison using multiple observational data in the Kuroshio Extension region. Acta Oceanologica Sinica, 2017, 36, 1-7.	1.0	10
41	CMODH Validation for C-Band Synthetic Aperture Radar HH Polarization Wind Retrieval Over the Ocean. IEEE Geoscience and Remote Sensing Letters, 2021, 18, 102-106.	3.1	10
42	On Modeling of Quadâ€Polarization Radar Scattering From the Ocean Surface With Breaking Waves. Journal of Geophysical Research: Oceans, 2020, 125, e2020JC016319.	2.6	9
43	Radar imaging of intense nonlinear Ekman divergence. Geophysical Research Letters, 2016, 43, 9810-9818.	4.0	8
44	Estimation of Sea Surface Current from X-Band Marine Radar Images by Cross-Spectrum Analysis. Remote Sensing, 2019, 11, 1031.	4.0	8
45	A geometrical optics model based on the non-Gaussian probability density distribution of sea surface slopes for wind speed retrieval at low incidence angles. International Journal of Remote Sensing, 2016, 37, 537-550.	2.9	7
46	Ocean Wind Retrieval Models for RADARSAT Constellation Mission Compact Polarimetry SAR. Remote Sensing, 2018, 10, 1938.	4.0	7
47	Observed Ocean Surface Winds and Mixed Layer Currents Under Tropical Cyclones: Asymmetric Characteristics. Journal of Geophysical Research: Oceans, 2022, 127, .	2.6	7
48	C-Band Right-Circular Polarization Ocean Wind Retrieval. IEEE Geoscience and Remote Sensing Letters, 2019, 16, 1398-1401.	3.1	6
49	A New Modulation Transfer Function With Range and Azimuth Dependence for Ocean Wave Spectra Retrieval From X-Band Marine Radar Observations. IEEE Geoscience and Remote Sensing Letters, 2017, 14, 1373-1377.	3.1	5
50	A C-band Geophysical Model Function for Determining Coastal Wind Speed Using Synthetic Aperture Radar. , 2018, , .		5
51	On C-Band Quad-Polarized Synthetic Aperture Radar Properties of Ocean Surface Currents. Remote Sensing, 2019, 11, 2321.	4.0	5
52	Compact Polarimetry Synthetic Aperture Radar Ocean Wind Retrieval: Model Development and Validation. Journal of Atmospheric and Oceanic Technology, 2021, 38, 747-757.	1.3	5
53	Validation of RADARSAT-2 Polarimetric SAR measurements of ocean waves. , 2009, , .		3
54	A new polarization ratio model from C-Band RADARSAT-2 fine Quad-Pol imagery. , 2010, , .		3

#	Article	IF	CITATIONS
55	Up-to-Downwave Asymmetry of the CFOSAT SWIM Fluctuation Spectrum for Wave Direction Ambiguity Removal. IEEE Transactions on Geoscience and Remote Sensing, 2022, 60, 1-12.	6.3	3
56	Estimating the Key Parameter of a Tropical Cyclone Wind Field Model over the Northwest Pacific Ocean: A Comparison between Neural Networks and Statistical Models. Remote Sensing, 2021, 13, 2653.	4.0	3
57	First Quasi-Synchronous Hurricane Quad-Polarization Observations by C-Band Radar Constellation Mission and RADARSAT-2. IEEE Transactions on Geoscience and Remote Sensing, 2022, 60, 1-10.	6.3	3
58	A Nonparametric Tropical Cyclone Wind Speed Estimation Model Based on Dual-Polarization SAR Observations. IEEE Transactions on Geoscience and Remote Sensing, 2022, 60, 1-13.	6.3	3
59	On polarimetric characteristics in SAR images of mesoscale cellular convection in the marine atmospheric boundary layer. Journal of Geophysical Research, 2011, 116, .	3.3	2
60	RADARSAT application in ocean wind measurements. , 2011, , .		2
61	Thermal front retreivals from SAR imagery. , 2012, , .		2
62	Marine oil slick and platform detection by compact polrimetric synthetic aperture radar. , 2016, , .		2
63	C-band Compact-Polarimetric SAR Monitoring of Ocean Winds. , 2019, , .		2
64	Air–Sea Interface Parameters and Heat Flux from Neural Network and Advanced Microwave Scanning Radiometer Observations. Remote Sensing, 2022, 14, 2364.	4.0	2
65	Observation of natural and artificial features on the sea surface from SAR satellite imagery with in-situ measurements. , 2011, , .		1
66	Recent development in SAR-derived winds using polarized RADARSAT-2 data. , 2013, , .		1
67	Tropical Cyclone Wind Direction Retrieval from C-Band Dual-Polarization Synthetic Aperture Radar. , 2018, , .		1
68	Synergistic Measurements of Hurricane Wind Speeds and Directions from C-band Dual-Polarization Synthetic Aperture Radar. , 2019, , .		1
69	Sea Surface Wind Retrieval Using the Combined Scatterometer and Altimeter Backscatter Measurements of the HY-2B Satellite. IEEE Transactions on Geoscience and Remote Sensing, 2022, 60, 1-12.	6.3	1
70	Ocean wave parameters retrieved directly from compact Polarimetric SAR data. Acta Oceanologica Sinica, 2022, 41, 129-137.	1.0	1
71	Breaking wave measurements with sar depolarized returns. , 2010, , .		0
72	Tropical cyclone vector winds from C-band dual-polarization synthetic aperture radar. , 2013, , .		0

#	Article	IF	CITATIONS
73	Hurricane tangential wind profile from synthetic aperture radar observations. , 2014, , .		0
74	A C-band cross polarization geophysical model function. , 2015, , .		0
75	Simultaneous multi-polarization SAR retrieval of ocean surface waves and winds from moderate to high states. , 2015, , .		0
76	Observation of tide from X-band marine radar image sequences. , 2016, , .		0
77	Non-Bragg scattering contributions to the dual-polarized SAR imaging of Hurricane Earl. , 2016, , .		0
78	Simulation and retrieval of CFOSAT at whitecap sea. , 2016, , .		0
79	The Construction of a Three-Dimensional Antenna Gain Matrix and Its Impact on Retrieving Sea Surface Mean Square Slope Based on Aircraft Wave Spectrometer Data. Journal of Atmospheric and Oceanic Technology, 2016, 33, 847-856.	1.3	0
80	Investigation of upper ocean response to typhoon kalmaegi (2014) using multiple satellites observation and numerical simulation. , 2017, , .		0
81	Upper Ocean Response of Yongxing Island Area to Typhoon â€~Kujira' in the South China Sea from Multiple-Satellite and Fixed-Point Observation. , 2018, , .		0
82	Examination of Typhoon Surface Wind Asymmetry in Northwest Pacific Ocean Using SMAP Observations. , 2019, , .		0
83	Multi-Scale, Multi-Frequency, and Quad-Polarized Microwave Scattering from Sea Surface Numerical Simulation. , 2019, , .		0
84	Contribution of Wave Breaking to Quad-Polarization Synthetic Aperture Radar. , 2019, , .		0
85	Interpreting Surface Ocean Phenomena Through Quad-Polarized SAR Measurements. , 2019, , .		0
86	Using Synthetic Aperture Radar and Radiometer Observations to Estimate Tropical Cyclone Wind Structure and Intensity. , 2021, , .		0
87	Synergistic Observations of Surface Winds and Currents in Tropical Cyclone. , 2021, , .		0
88	Aircraft and Satellite Observations of Vortex Evolution and Surface Wind Asymmetry of Concentric Eyewalls in Hurricane Irma. Remote Sensing, 2022, 14, 2158.	4.0	0